7N-18
198518
P-33

NASA TN D-254

TECHNICAL NOTE
D-254

AN ANALYSIS OF NOSE ABLATION FOR BALLISTIC VEHICLES

By Leonard Roberts

Langley Research Center
Langley Field, Va.

NATIONAL AERONAUTICS AND SPACE ADMINISTRATION

WASHINGTON April 1960

ERRATA

NASA Technical Note D-254

By Leonard Roberts
April 1960

Page 11: On the right-hand sides of equations (19), (20), and (21), the signs of the exponents of R should be plus instead of minus. The corrected equations therefore are:

$$\frac{Q_r}{Q_0} \approx \frac{2ep}{K_p}(\rho^*)^{-p}V_i^{-3}\left[\frac{1 - e^{-B/2}}{\bar{H}_p(B)}\right]R^{(1-p)}\epsilon\left(\frac{T_a}{10^3}\right)^4 \tag{19}$$

For laminar heating

$$\left(\frac{Q_r}{Q_0}\right)_{lam} \approx 1.5\left[\frac{V_i}{(gr)^{1/2}}\right]^{-3}\left[\frac{1 - e^{-B/2}}{\bar{H}_{1/2}(B)}\right]R^{1/2}\epsilon\left(\frac{T_a}{10^4}\right)^4 \tag{20}$$

and for turbulent heating

$$\left(\frac{Q_r}{Q_0}\right)_{turb} \approx 0.3\left[\frac{V_i}{(gr)^{1/2}}\right]^{-3}\left[\frac{1 - e^{-B/2}}{\bar{H}_{4/5}(B)}\right]R^{1/5}\epsilon\left(\frac{T_a}{10^4}\right)^4 \tag{21}$$

Page 22, lines 5 and 6: The values of m and d at the sonic point should be corrected as follows:

$$m = 39.9 \text{ lb/sq ft}$$

$$d = 3.3 \text{ in.}$$

Page 23, next line from last: The value 1.5 inches should be 3.3 inches.

Page 30: In figure 4, the two dimensions labeled 1.5 in. should be changed to 3.3 in., and the dashed line indicating the change of shape should be altered accordingly.

NASA-Langley, 1961

Issued 11-17-61

lV

NATIONAL AERONAUTICS AND SPACE ADMINISTRATION

TECHNICAL NOTE D-254

AN ANALYSIS OF NOSE ABLATION FOR BALLISTIC VEHICLES

By Leonard Roberts

SUMMARY

L856

A simplified analysis is made of the ablation experienced by ballistic vehicles. It is found in general that the heat lost by radiation is negligible compared with that disposed by ablation. A limiting total mass loss is found which is independent of vehicle weight and drag and independent of initial and impact velocity.

Expressions are presented from which may be calculated the total mass loss experienced by the nose of the vehicle at both the stagnation point, where laminar flow prevails and at the sonic point, where the flow is considered turbulent. A typical calculation shows the change in shape of a hemispherical nose during reentry.

INTRODUCTION

The effectiveness of a long-range ballistic vehicle depends largely on its impact velocity. If such a vehicle is to avoid wind drift, it must maintain high velocity even down to low altitudes.

One of the foremost problems associated with such a vehicle is the disposal of excess energy in the form of heat, the rate of disposal of this heat rather than the total amount being the main consideration.

The most efficient way to dispose of heat at such high rates is to provide the vehicle with a shield of material of high thermal capacity, and since the thermal capacity of metals is limited, materials which undergo ablation have been used. The removal of material from the surface of the shield during ablation is accompanied by a large loss of heat; part of the heat is absorbed by the phase change and part by the additional heating of the ablation products in the boundary layer. (See, for example, refs. 1 to 4.)

An analysis of the ablation experienced by reentry vehicles requires a knowledge of the motion and heating experience of the vehicle. This information is provided by the analyses of references 5 and 6, in which were derived expressions for the heating rates and total heat input.

The purpose of the present report is to derive engineering-type expressions for the ablation experienced by a ballistic-vehicle shield near the stagnation and sonic points during reentry into the atmosphere. In view of the beneficial effects of mass addition into the boundary layer, the type of ablation considered herein is that in which there is no liquid film; the material undergoes sublimation at the surface and thereafter flows over the nose in the boundary layer. The methods applied to the ablation problem for manned reentry in reference 7 are used to obtain simple expressions from which may be calculated the total mass loss and the insulation requirements for any vehicle.

L 8 5 6

SYMBOLS

A	reference area for drag, sq ft
a	acceleration, ft/sec^2
B	ballistic-impact parameter
C_D	drag coefficient
c	specific heat, Btu/(lb)($^\circ$R)
d	ablated thickness, in.
$\bar{G}$	mean dimensionless enthalpy
g	gravitational acceleration, ft/sec^2
$\bar{H}$	dimensionless total heat input
H_{eff}	effective heat capacity, Btu/lb
h	altitude, ft
J	mechanical equivalent of heat, 778 ft-lb/Btu
K	convective heating coefficient
k	thermal conductivity, Btu/(ft)(sec)($^\circ$R)
L	latent heat of sublimation, Btu/lb
l	characteristic length of vehicle, ft

M	mass of vehicle, slugs
m	mass ablated, lb/sq ft
N_{Pr}	Prandtl number
N_{Sc}	Schmidt number
p	1/2 at laminar stagnation point, 4/5 at turbulent sonic point
Q	total convective heat input, Btu/sq ft
q	local convective heat-transfer rate, Btu/(sq ft)(sec)
R	radius of curvature of nose, ft
R_∞	Reynolds number, $\frac{\rho_\infty V l}{\mu_\infty}$
r	radius of earth, ft
T	temperature, $^{\circ}R$
t	time, sec
u	horizontal-velocity component, ft/sec
$\bar{u} = \frac{u}{V_c}$	
V	total velocity, ft/sec
V_c	circular velocity, $(gr)^{1/2} = 26{,}000$ ft/sec
$v = \frac{V}{V_i}$	
w	concentration of shield material in gaseous form
Z	dimensionless function of $\bar{u}$ determined by equation (1)
z	outward normal distance from ablation surface, ft
α	fractional temperature rise of gaseous material

L
8
5
6

β	atmospheric density decay parameter, ft^{-1}
γ	flight-path angle relative to local horizontal, deg
ϵ	emissivity
η	fractional decrease in mass loss due to internal shielding
θ	integral thickness of heated layer in solid shield, ft
λ	ablation shielding parameter
μ	coefficient of dynamic viscosity, slugs/ft-sec
ρ	density, slugs/cu ft
σ	Stefan-Boltzmann constant 5×10^{-13} Btu ft^{-2} sec^{-1} $^{o}R^{-4}$

L
8
5
6

Subscripts:

a	sublimation condition
b	solid shield condition
e	external to gas boundary layer
f	final, or impact, condition
i	initial condition
ins	insulation
lam	laminar
max	maximum
r	radiation
s	surface condition
turb	turbulent
1	gas produced by sublimation
2	air in boundary layer

0	no sublimation
∞	free stream

Superscripts:

'	differentiation with respect to $\bar{u}$
-	dimensionless quantity
*	sea level
~	mean quantity

L 8 5 6

ANALYSIS

Motion and Heating

A generalized analysis of reentry into planetary atmospheres has been made in reference 6 where expressions for laminar and turbulent convective heating rates were obtained. Those expressions were presented in a form which makes a study of ablation during reentry a fairly simple matter as shown in reference 7. In the notation of reference 6, the equation of motion of a nonlifting ballistic vehicle is written

$$uZ'' + (\beta r)^{1/2}\sin\gamma = 0 \tag{1}$$

where

$$\left.\begin{aligned} Z &= \frac{\rho_\infty}{2\dfrac{M}{C_D A}}\left(\frac{r}{\beta}\right)^{1/2}\bar{u} \\ \rho_\infty &= \rho^* e^{-\beta h} \\ \frac{u}{V_c} &= \frac{u}{(gr)^{1/2}} = \bar{u} \end{aligned}\right\} \tag{2}$$

The solution of equation (1) is written

$$Z = -\bar{u}\log_e\frac{\bar{u}}{\bar{u}_i}(\beta r)^{1/2}\sin\gamma \tag{3}$$

where $\bar{u}_i$ is the initial dimensionless horizontal component of velocity determined from the vehicle trajectory before reentry.

The motion and heating history of reentry vehicles has been described in reference 6 in terms of the functions $Z(\bar{u})$, and general expressions for the primary quantities of interest (for example, maximum deceleration and maximum heating rate) were presented therein. The results of references 5 and 6 will be expressed herein in terms of total velocity V rather than the horizontal component u through

L
8
5
6

$$\left.\begin{aligned} V &= \frac{u}{\cos\gamma} \\ v &= \frac{V}{V_i} = \frac{\bar{u}}{\bar{u}_i} \end{aligned}\right\} \tag{4}$$

and in terms of the parameters $\frac{M}{C_D A}$, V_i, and γ.

Impact velocity.- The first quantity of interest for a ballistic vehicle is the impact velocity V_f, which is most easily obtained from the density-velocity relation

$$\frac{\rho_\infty}{\rho^*} = \frac{2}{\rho^*}\left(\frac{\beta}{r}\right)^{1/2} \frac{M}{C_D A} \frac{Z}{\bar{u}} \tag{5}$$

and equations (3) and (4). In terms of a ballistic impact parameter

$$B = \left(\frac{\beta}{\rho^*} \frac{M}{C_D A} \sin\gamma\right)^{-1} \tag{6}$$

equation (5) with $\frac{\rho_\infty}{\rho^*} = 1$ and $V = V_f$ is written

$$v_f = e^{-\frac{1}{2}B} \tag{7}$$

The variation of B with v_f is shown in figure 1. The parameter B which is used to characterize trajectories in reference 5 may be interpreted physically as

$$B = \frac{\frac{C_DA}{\sin\gamma}\frac{\rho^*}{\beta}}{M}$$

$$= \frac{C_DA\int_0^\infty \rho_\infty \, d\left(\frac{h}{\sin\gamma}\right)}{M}$$

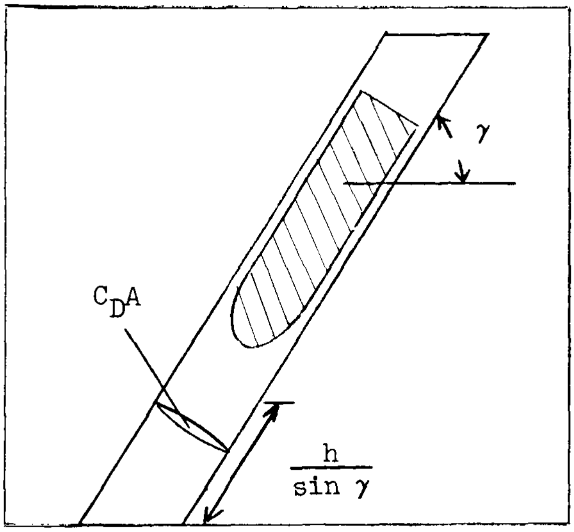

$$= \frac{\text{Mass of column of air in vehicle path}}{\text{Mass of vehicle}} \tag{8}$$

(where the parameter C_DA is interpreted as the effective area of cross section of the vehicle).

Equation (7) shows that the impact velocity increases as B decreases, a result to be expected in view of the foregoing interpretation of B.

<u>Maximum deceleration</u>.- As shown in reference 5, the deceleration is written

$$-a = -\beta V_i^2 \sin\gamma \; v^2 \log_e v \tag{9}$$

which has a maximum value

$$-a_{max} = \frac{\beta V_i^2}{2e} \sin\gamma$$

at $v = e^{-\frac{1}{2}}$. Thus, the vehicle will experience maximum deceleration before impact if $B \geqq 1$, but it will experience increasing deceleration up to impact if $B < 1$.

<u>Convective laminar and turbulent heating</u>.- The general expression for the heating rate is

$$q_0 = \frac{K_p}{R^{1-p}} \rho^p V^3 \tag{10}$$

where, for laminar flow, at the stagnation point

$$\left.\begin{aligned} p &= \frac{1}{2} \\ K_p &= 2 \times 10^{-8} \end{aligned}\right\} \tag{11a}$$

and for turbulent flow, at the sonic point

$$\left.\begin{aligned} p &= \frac{4}{5} \\ K_p &= 9 \times 10^{-7} \end{aligned}\right\} \tag{11b}$$

L
8
5
6

Equation (10) may be expressed in terms of Z and $\bar{u}$ as

$$q_0 = \frac{2^p K_p}{R^{1-p}} \left(\frac{M}{C_D A}\right)^p \left(\frac{\beta}{r}\right)^{p/2} \frac{(gr)^{3/2}}{\cos^3\gamma} \bar{q}_0 \frac{\text{Btu}}{(\text{sq ft})(\text{sec})} \tag{12}$$

where

$$\bar{q}_0 = \bar{u}^3 \left(\frac{Z}{\bar{u}}\right)^p \tag{13}$$

Equations (12) and (13) may be rewritten in terms of v and B as

$$q_0 = \frac{2^p K_p}{R^{1-p}} (\rho^*)^p B^{-p} V_i{}^3 v^3 (-\log_e v)^p \tag{14}$$

The relation between velocity and time required to integrate equation (14) is found from equation (9)

$$a = V_i \frac{dv}{dt} = \beta V_i{}^2 \sin\gamma \; v^2 \log_e v$$

or

$$\frac{dv}{dt} = V_i \beta \sin\gamma \; v^2 \log_e v$$

Integration of equation (14) with respect to t then gives

$$Q_0 = \frac{2^p K_p}{R^{1-p}} \frac{(\rho^*)^p B^{-p}}{\beta \sin \gamma} V_i^2 \int_{v_f}^{1} v(-\log_e v)^{p-1} dv$$

$$= \frac{K_p}{R^{1-p}} (\rho^*)^p (p\beta \sin \gamma)^{-1} V_i^2 \overline{H}_p(B) \tag{15}$$

L-856

where

$$\overline{H}_p(B) = pB^{-p}\Gamma_B(p) \tag{16}$$

and $\Gamma_B(p)$ is the incomplete gamma function. The function $\overline{H}_p(B)$ is shown in figure 2 and lies in the range $0 \leqq \overline{H}_p \leqq 1$. In particular when $p = \frac{1}{2}$ and $B \rightarrow \infty$

$$\overline{H}_{1/2} \rightarrow \frac{1}{2} B^{-\frac{1}{2}} \Gamma\left(\frac{1}{2}\right)$$

and the expression for the total heat input in reference 6

$$Q_0 = \frac{K_{1/2}}{R^{1/2}} \frac{V_i^2}{\beta \sin \gamma} \left(\frac{M}{C_D A}\right)^{1/2} \Gamma\left(\frac{1}{2}\right)$$

is recovered.

The maximum heating rate is found from equation (14); the maximum value of $v^3(-\log_e v)^p$ occurs at $v = e^{-p/3}$ and gives

$$\left(q_0\right)_{max} = \frac{2^p K_p}{R^{1-p}} (\rho^*)^p B^{-p} V_i^3 \left(\frac{3e}{p}\right)^{-p} \tag{17}$$

It is seen that maximum heating occurs before maximum deceleration $\left(v = e^{-1/2}\right)$ for both laminar and turbulent heating.

Reynolds number.- The Reynolds number is also written in terms of the parameter B as

$$\frac{R_\infty}{l} = \frac{V\rho_\infty}{\mu_\infty} = \frac{2(\beta g)^{1/2}}{\mu_\infty \cos\gamma}\frac{M}{C_D A} Z = \frac{2}{B}\frac{\rho^* V_i}{\mu_\infty}(-v \log_e v)$$

The maximum value of the Reynolds number occurs at $V = e^{-1}$ and is written

$$\left(\frac{R_\infty}{l}\right)_{max} = \frac{2}{Be}\frac{\rho^* V_i}{\mu_\infty} = \frac{2}{B} e^{\frac{1}{2}B-1} \frac{\rho^* V_f}{\mu_\infty}$$

and it may be verified that

$$\left(\frac{R_\infty}{l}\right)_{max} \geqq \frac{\rho^* V_f}{\mu_\infty}$$

that is, the maximum value is greater than or equal to the sea-level or impact value, (equality when $B = 2$). Alternately in terms of the circular velocity $(gr)^{1/2} = 26{,}000$ ft/sec

$$\left(\frac{R_\infty}{l}\right)_{max} = \frac{130}{B}\frac{V_i}{(gr)^{1/2}} \times 10^6 \text{ ft}^{-1} \tag{18}$$

In order to insure a high impact velocity V_f given by

$$V_f = V_i e^{-\frac{1}{2}B}$$

it is necessary that V_i be large and B small. The occurrence of turbulent flow therefore cannot be avoided as is seen from equation (18).

<u>Surface radiation</u>.- Ballistic reentry is typified by high convective heating rates and short duration, and it is to be expected that the heat loss by radiation is negligible compared with the convective input Q_0. An estimate of the ratio

$$\frac{\text{Total heat loss by radiation}}{\text{Total convective heat input}}$$

is easily obtained as follows: The duration of reentry is approximately, from equations (7) and (9),

L
8
5
6

$$\frac{V_i - V_f}{\frac{1}{2}\left(-a_{max}\right)} = 4e\left(1 - e^{-B/2}\right)\left(V_i\beta \sin \gamma\right)^{-1}$$

and the total heat loss by radiation is approximately

$$Q_r = 4e\left(1 - e^{-B/2}\right)\left(V_i\beta \sin \gamma\right)^{-1}\sigma\epsilon T_a{}^4$$

$$= 2e\left(1 - e^{-B/2}\right)\left(V_i\beta \sin \gamma\right)^{-1}\epsilon\left(\frac{T_a}{10^3}\right)^4$$

L856

where the numerical value $\frac{1}{2} \times 10^{-12}$ Btu ft^{-2} sec^{-1} $^{\circ}$R has been used for the Stefan-Boltzmann constant σ.

Thus, by using the expressions for Q_0 given by equation (15), the ratio Q_r/Q_0 is written as

$$\frac{Q_r}{Q_0} \approx \frac{2ep}{K_p}(\rho*)^{-p}V_i{}^{-3}\left[\frac{1 - e^{-B/2}}{\overline{H}_p(B)}\right]R^{-(1-p)}\epsilon\left(\frac{T_a}{10^3}\right)^4 \tag{19}$$

For laminar heating

$$\left(\frac{Q_r}{Q_0}\right)_{lam} \approx 1.5\left[\frac{V_i}{(gr)^{1/2}}\right]^{-3}\left[\frac{1 - e^{-B/2}}{\overline{H}_{1/2}(B)}\right]R^{-1/2}\epsilon\left(\frac{T_a}{10^4}\right)^4 \tag{20}$$

and for turbulent heating

$$\left(\frac{Q_r}{Q_0}\right)_{turb} \approx 0.3\left[\frac{V_i}{(gr)^{1/2}}\right]^{-3}\left[\frac{1 - e^{-B/2}}{\overline{H}_{4/5}(B)}\right]R^{-1/5}\epsilon\left(\frac{T_a}{10^4}\right)^4 \tag{21}$$

When typical values

$$B = 5 \qquad \frac{V_i}{(gr)^{1/2}} = 1$$

$$R = 1 \qquad \epsilon = 1/2$$

are inserted, equations (20) and (21) give

$$\left(\frac{Q_r}{Q_0}\right)_{lam} \approx 2\left(\frac{T_a}{10^4}\right)^4$$

and

$$\left(\frac{Q_r}{Q_0}\right)_{turb} \approx 0.8\left(\frac{T_a}{10^4}\right)^4$$

L
8
5
6

Thus, even for mean values of T_a of the order of $4,000^\circ$ R to $5,000^\circ$ R, the heat lost by radiative cooling is of the order of 5 to 10 percent for laminar flow and even less for turbulent flow.

For vehicles of higher impact velocity (therefore, large V_i and small B) the heat loss by radiation becomes a decreasingly small fraction of the total convective heat input, as may be seen from the form of equations (20) and (21). In the following analysis, therefore, radiation from the surface is neglected.

Sublimation and Heat Accumulation

The equations used herein to determine mass loss and accumulation of heat are those developed in reference 7; briefly they are written

$$\underbrace{q_0}_{\substack{\text{Heating rate}\\ \text{for no}\\ \text{ablation}}} = \underbrace{\left[c_b\left(T_a - T_b\right) + L + \alpha_p\tilde{c}_p\left(T_e - T_a\right)\right]\frac{dm}{dt}}_{\substack{\text{Rate of disposal of heat}\\ \text{by mass loss}}} + \underbrace{\rho_b c_b \frac{d}{dt}\left[\left(T_s - T_b\right)\theta\right]}_{\substack{\text{Rate of accumulation}\\ \text{of heat by shield}}} \tag{22}$$

In equation (22) θ is an integral heated thickness

$$\theta = \int_{-\infty}^{0} \frac{T - T_b}{T_s - T_b}\, dz \tag{23}$$

α is the fractional increase in temperature of the gas products of sublimation, and $\tilde{c}_p$ is the mean specific heat of the gas mixture in the boundary layer

$$\tilde{c}_p = c_{p,1}\tilde{w} + c_{p,2}(1 - \tilde{w}) \tag{24}$$

where $\tilde{w}$ is the effective concentration of the shield material in gaseous form and is given as a function of Schmidt number in reference 2.

The heating rate q_0 has already been given in terms of the dimensionless velocity v, and the enthalpy $c_{p,2}\left(T_e - T_a\right)$ is also easily expressed in terms of v

L
3
5
5

$$c_{p,2}\left(T_e - T_a\right) \approx c_{p,2}\left(T_e - T_b\right) = \frac{1}{2}\frac{V_i^2}{gJ}v^2 \tag{25}$$

Since the purpose of the ablation shield is to dispose of rather than accumulate heat it may be expected that the second term on the right of equation (22) will be small compared with the first term; thus, when the second term is ignored

$$\frac{dm}{dt} = \frac{q_0}{L + \alpha_p\tilde{c}_p\left(T_e - T_a\right) + c_b\left(T_a - T_b\right)} \tag{26}$$

As in reference 7 the rate of mass loss is expressed in terms of the vehicle velocity V and the explicit dependence on the time t is eliminated, thus equation (26) is written

$$\frac{dm}{dt} = \frac{2^p K_p(\rho*)^p B^{-p} V_i}{\dfrac{R^{1-p}}{2}\,\dfrac{\alpha_p}{gJ}\,\dfrac{\tilde{c}_p}{c_{p,2}}}\, v(-\log_e v)^p\left(1 - \frac{\lambda}{v^2 + \lambda}\right) \tag{27}$$

where

$$\lambda = \frac{L + c_b\left(T_a - T_b\right)}{\dfrac{1}{2}\dfrac{V_i^2}{gJ}\alpha_p\dfrac{\tilde{c}_p}{c_{p,2}}} = \frac{\text{Maximum internal shielding enthalpy}}{\text{Maximum external shielding enthalpy}} \tag{28}$$

The maximum mass loss rate will depend on λ. When λ is small, this maximum occurs at $v = e^{-p}$; but when λ is large, it occurs at $v = e^{-p/3}$ and coincides with peak heating.

Mass loss.- The total mass loss experienced by the shield during reentry is found by integration of equation (27) and gives

$$m = \frac{\dfrac{2^p K_p}{R^{1-p}}(\rho*)^p B^{-p}}{\dfrac{1}{2}\dfrac{\alpha_p}{gJ}\dfrac{\tilde{c}_p}{c_{p,2}}(\beta \sin \gamma)} \int_{v_f}^{1} \frac{1}{v}(-\log_e v)^{p-1}\left(1 - \frac{\lambda}{v^2 + \lambda}\right)dv$$

$$= \frac{\dfrac{K_p}{R^{1-p}}(\rho*)^p}{\dfrac{1}{2}\dfrac{\alpha_p}{gJ}\dfrac{\tilde{c}_p}{c_{p,2}} p\beta \sin \gamma}(1 - \eta) \text{ lb/sq ft} \tag{29}$$

L
8
5
6

where

$$\eta = \frac{\displaystyle\int_{v_f}^{1}\left(\frac{\lambda}{v^2 + \lambda}\right)\frac{1}{v}(-\log_e v)^{p-1}dv}{\displaystyle\int_{v_f}^{1} \frac{1}{v}(-\log_e v)^{p-1}dv} \tag{30}$$

The quantity η which represents the reduction in mass loss due to internal shielding is found by evaluating the integrals in equation (30) and is given approximately by

$$\eta = \left(\frac{\lambda}{1 + \lambda}\right)^{\overline{H}_p} \tag{31}$$

(The numerical evaluation of equation (30) agrees with equation (31) to within a few percent.)

The general approximate form for η given by equation (31) is suggested by a similar result derived in reference 7.

By combining equations (29) and (31), the total mass loss may be written

$$m = \frac{\dfrac{K_p}{R^{1-p}}(\rho*)^p(p\beta \sin \gamma)^{-1}{V_i}^2\overline{H}_p}{L + c_b\left(T_a - T_b\right) + \dfrac{1}{2}\dfrac{{V_i}^2}{gJ}\alpha_p\dfrac{\tilde{c}_p}{c_{p,2}}\overline{G}_p} \text{ lb/sq ft} \tag{32}$$

where

$$\bar{G}_p = \bar{H}_p \left\{ \left[1 - \left(\frac{\lambda}{1 + \lambda} \right)^{\bar{H}_p} \right]^{-1} - \frac{\lambda}{\bar{H}_p} \right\} \tag{33}$$

The significance of the function $\bar{G}_p$ is discussed later.

When the internal shielding is negligible compared with the gas-layer shielding $(\lambda \to 0)$, equation (32) reduces to

$$m = \frac{\frac{K_p}{R^{1-p}} (\rho *)^p (p\beta \sin \gamma)^{-1}}{\frac{1}{2} \frac{\alpha_p}{gJ} \frac{\tilde{c}_p}{c_{p,2}}} \text{ lb/sq ft} \tag{34}$$

It is interesting to note that this upper limit is independent of the ballistic parameter $\frac{M}{C_D A}$, the entry velocity V_i, and the impact velocity V_f.

On the other hand, when the gas-layer shielding is negligible compared with the internal shielding $(\lambda \to \infty)$, the mass loss tends to the limit

$$m = \frac{K_p}{R^{1-p}} (\rho *)^p \frac{(p\beta \sin \gamma)^{-1} V_i^2}{L + c_b \left(T_a - T_b \right)} \bar{H}_p \tag{35}$$

which depends on V_i and the impact parameter B through $\bar{H}_p$. This latter limit also applies to a heat sink when $L = 0$, the thermal capacity then being $c_b \left(T_a - T_b \right)$ Btu/lb. In general, for an ablation shield neither the internal shielding nor the gas-layer shielding is negligible and the mass loss given by equation (32) is less than either of the limiting values obtained from equations (34) or (35).

Effective heat capacity.- The effective heat capacity or heat of ablation at any time during reentry is a function primarily of the stream enthalpy and therefore the vehicle speed. When the entire trajectory is considered however the more appropriate definition is

$$H_{eff} = \frac{\text{Total heat disposed by ablation}}{\text{Total mass loss}} = \frac{Q_O}{m}$$

when the accumulation of heat is neglected. By using the expressions for Q_O and m given by equations (15) and (32), respectively, H_{eff} may be written

$$H_{eff} = L + c_b\left(T_a - T_b\right) + \frac{1}{2}\frac{V_i^{2}}{gJ}\alpha_p\frac{\tilde{c}_p}{c_{p,2}}\bar{G}_p \tag{36}$$

where

$$\bar{G}_p = \bar{H}_p\left\{\left[1 - \left(\frac{\lambda}{1 + \lambda}\right)^{\bar{H}_p}\right]^{-1} - \frac{\lambda}{\bar{H}_p}\right\} \tag{37}$$

The form of equation (36) is such that $\frac{1}{2}\frac{V_i^{2}}{gJ}\bar{G}_p$ may be interpreted as L856
the mean stream enthalpy during reentry. It is interesting to note that $\bar{G}_p$ is a function of λ. For very small impact velocities, $v_f \approx 0$; then

$$\bar{H}_p \rightarrow 0$$

and

$$\bar{G}_p \rightarrow \left(\log\frac{1 + \lambda}{\lambda}\right)^{-1} - \lambda$$

independently of p. For large impact velocities, $v_f \rightarrow 1$, and $\bar{G}_p \rightarrow 1$ for all values of λ. Figure 3 shows this range of variation of $\bar{G}_p$. For a fixed value of v_f (and, therefore, a fixed value of $\bar{H}_p$)

$$\bar{H}_p \leqq G_p \leqq \frac{1}{2}\left(\bar{H}_p + 1\right) \tag{38}$$

with the lower limit corresponding to $\lambda = 0$ and the upper limit corresponding to $\lambda \rightarrow \infty$.

In order to determine the suitability of a material for use as an ablation shield, consideration must be given to the amount of insulation material. The total weight of the shield required to ensure a given back-surface temperature is the sum of the weight required for ablation and that required for insulation.

It was shown in reference 7 that an upper limit to the insulation requirements may be obtained by assuming that the surface temperature is constant and equal to the ablation temperature throughout reentry and by ignoring the effect of ablation on the temperature distribution. With the foregoing approximations, the appropriate solution of the heat-conduction equation for a thermally thick shield is written

$$\frac{T - T_b}{T_a - T_b} = \mathrm{erfc}\left[-\left(\frac{\rho_b c_b}{k_b t}\right)^{1/2}\frac{z}{2}\right] \tag{39}$$

The temperature distribution $T(z)$ at impact is obtained from equation (39) by inserting the value t_f. An upper limit to the heat accumulated by the shield is found by integration of equation (39) and gives

$$Q_f = \rho_b c_b\left(T_a - T_b\right)\theta = \frac{2}{\pi^{1/2}}\left(\rho_b c_b k_b\right)^{1/2}\left(T_a - T_b\right)t_f^{1/2} \tag{40}$$

so that

$$\theta_f = \frac{2}{\pi^{1/2}}\left(\frac{k_b t_f}{\rho_b c_b}\right)^{1/2}$$

It is seen that the expressions for the temperature distribution and accumulation of heat depend primarily on the properties of the solid shield. The ballistic characteristics enter only through the factor $t_f^{1/2}$.

Numerical Calculations

General expressions have been derived from which the mass loss during reentry and the overall effective heat capacity may be determined. In order to use equations (32) and (36), the quantities α_p, $\frac{\tilde{c}_p}{c_{p,2}} = \frac{c_{p,1}}{c_{p,2}}\tilde{w} + 1 - \tilde{w}$, and $\overline{H}_p$ must be known.

For laminar flow with $N_{Pr} = N_{Sc} = 0.7$ the results of reference 2 give

$$\alpha_p \approx 3/5 \quad \text{and} \quad \tilde{w} \approx 5/6$$

For turbulent flow, the values

$$\alpha_p = 3/10 \quad \text{and} \quad \tilde{w} = 5/6$$

give good agreement with the experimental results of reference 8 both for air and helium injections into the boundary layer. More generally, equations (32) and (36) may be used in conjunction with experimentally determined values of the quantity $\alpha_p\tilde{c}_p/c_{p,2}$ for the particular material under consideration.

The shielding parameter λ may now be written

For laminar flow:

$$\lambda = \frac{L + c_b(T_a - T_b)}{8{,}100\left(\frac{V_i^2}{gr}\right)\left(\frac{5}{6}\frac{c_{p,1}}{c_{p,2}} + \frac{1}{6}\right)} \tag{41a}$$

L 856

For turbulent flow:

$$\lambda = \frac{L + c_b(T_a - T_b)}{4{,}050\left(\frac{V_i^2}{gr}\right)\left(\frac{5}{6}\frac{c_{p,1}}{c_{p,2}} + \frac{1}{6}\right)} \tag{41b}$$

It is seen that for given values of quantities contained in λ, the turbulent value of λ is twice the laminar value. The foregoing expressions for $\alpha_p\tilde{c}_p/c_{p,2}$ and λ used in conjunction with equation (32) provide a simple determination of the mass loss. When the appropriate values of K_p, p, λ, $\rho^* = 0.0027$ slugs/cu ft, and $\beta = 23{,}500\ \text{ft}^{-1}$ are inserted, equation (32) reduces to the following:

For laminar flow:

$$m = \frac{33{,}000\left(\frac{V_i^2}{gr}\right)R^{-1/2}(\sin\gamma)^{-1}\bar{H}_{1/2}}{L + c_b(T_a - T_b) + 8{,}100\left(\frac{5}{6}\frac{c_{p,1}}{c_{p,2}} + \frac{1}{6}\right)\left(\frac{V_i^2}{gr}\right)\bar{G}_{1/2}}\ \text{lb/sq ft} \tag{42a}$$

and for turbulent flow:

$$m = \frac{160{,}000\left(\frac{V_i^2}{gr}\right)R^{-1/5}(\sin\gamma)^{-1}\bar{H}_{4/5}}{L + c_b(T_a - T_b) + 4{,}050\left(\frac{5}{6}\frac{c_{p,1}}{c_{p,2}} + \frac{1}{6}\right)\left(\frac{V_i^2}{gr}\right)\bar{G}_{4/5}}\ \text{lb/sq ft} \tag{42b}$$

Similarly, the effective heat capacity is written, from equation (36) for laminar flow

$$H_{eff} = L + c_b\left(T_a - T_b\right) + 8{,}100\left(\frac{5}{6}\,\frac{c_{p,1}}{c_{p,2}} + \frac{1}{6}\right)\frac{V_i^{\,2}}{gr}\,\overline{G}_{1/2}\ \text{Btu/lb} \qquad (43a)$$

and for turbulent flow

$$H_{eff} = L + c_b\left(T_a - T_b\right) + 4{,}050\left(\frac{5}{6}\,\frac{c_{p,1}}{c_{p,2}} + \frac{1}{6}\right)\frac{V_i^{\,2}}{gr}\,\overline{G}_{4/5}\ \text{Btu/lb} \qquad (43b)$$

The functions $\overline{H}_p$ and $\overline{G}_p$ which appear in equations (42a) to (43b) are defined by equations (16) and (33), respectively. The function $\overline{H}_p$ is extremely well approximated as follows:

$$\overline{H}_p \approx \left(-2 \log_e v_f\right)^{-p}\Gamma(p + 1) \qquad \text{for} \quad v_f < 0.15$$

and

$$\overline{H}_p \approx \left(1 - \omega_p\right) + \omega_p v_f \qquad \text{for} \quad v_f > 0.15$$

or for laminar flow

$$\left.\begin{aligned} \overline{H}_{1/2} &\approx 0.886\left(-2 \log_e v_f\right)^{-1/2} && v_f < 0.15 \\ \overline{H}_{1/2} &\approx 0.35 + 0.65 v_f && v_f > 0.15 \end{aligned}\right\} \qquad (44a)$$

and for turbulent flow

$$\left.\begin{aligned} \overline{H}_{4/5} &\approx 0.931\left(-2 \log_e v_f\right)^{-4/5} && v_f < 0.15 \\ \overline{H}_{4/5} &\approx 0.20 + 0.80 v_f && v_f > 0.15 \end{aligned}\right\} \qquad (44b)$$

The dimensionless impact velocity v_f is determined easily from equation (7), that is

$$v_f = e^{-\frac{1}{2}B}$$

The function $\overline{G}_p$ may be determined from equation (33) by using the foregoing expressions for λ and $\overline{H}_p$.

It is seen from figures 3(a) and 3(b) that for $0.05 < v_f < 0.15$ there is little variation of $\overline{G}_p$ with v_f and that $\overline{G}_p$ does not vary appreciably with λ for $\lambda > 0.15$ for laminar flow and $\lambda > 0.50$ for turbulent flow. (This range of λ corresponds roughly to $L + c_b\left(T_a - T_b\right) > 1{,}000$ Btu/lb when $\frac{V_i{}^2}{gr}\left(\frac{5}{6}\frac{c_{p,1}}{c_{p,2}} + \frac{1}{6}\right) \approx 1.$) Thus, as a first approximation the function $\overline{G}_p$ can be replaced by the numerical value 0.6.

An estimate of the amount of insulation is made by writing equation (39) in the approximate form, at $t = t_f$

$$\frac{T - T_b}{T_a - T_b} \approx e^{z/\theta_f} \tag{45}$$

where

$$\theta_f = \frac{2}{\pi^{1/2}}\left(\frac{k_b t_f}{\rho_b c_b}\right)^{1/2}$$

and writing

$$t_f \approx \frac{V_i - V_f}{\frac{1}{2}\left(-a_{max}\right)} = \frac{4e\left(1 - v_f\right)}{V_i \beta \sin \gamma} \approx \frac{4e}{V_i \beta \sin \gamma} \tag{46}$$

Equation (45) then reads

$$-\rho_b z = \frac{2}{\pi^{1/2}}\left(\frac{\rho_b k_b}{c_b}\right)^{1/2}\left(\frac{4e}{V_i \beta \sin \gamma}\right)^{1/2}\log_e\left(\frac{T_a - T_b}{T - T_b}\right)$$

Thus, if at the start of reentry the back surface temperature is T_b and it is required to limit the temperature to T_f, the amount of insulation is given by

$$m_{ins} = \frac{2}{\pi^{1/2}}\left(\frac{\rho_b k_b}{c_b}\right)^{1/2}\left(\frac{4e}{V_i \beta \sin \gamma}\right)^{1/2}\log_e\left(\frac{T_a - T_b}{T_f - T_b}\right) \tag{47}$$

It is seen from equation (47) that the amount of insulation is reduced by choosing a material such that $\frac{\rho_b k_b}{c_b}$ and $\left(T_a - T_f\right)$ are small. Typical values

$$T_a - T_b = 1{,}000^\circ \text{ R} \qquad V_i\beta = 1 \text{ sec}^{-1}$$

$$T_f - T_b = 300^\circ \text{ R} \qquad \gamma = 30^\circ$$

$$\left(\frac{\rho_b k_b}{c_b}\right)^{1/2} = 10^{-1} \text{ lb/(sq ft)}\left(\text{sec}^{1/2}\right)$$

give

L 8 5 6

$$m_{ins} = 0.56 \text{ lb/sq ft}$$

If $T_a - T_b$ is increased to 4,000° R the result is an increase of m_{ins} to 1.21 lb/sq ft.

Change of Shape

An important consideration in the design of an ablation shield is the change in shape of the shield during reentry. For slender but blunt nosed vehicles the stagnation point and sonic point may be located fairly close to each other but nevertheless experience quite different heating histories. The recession distances at these two points may differ considerably, therefore, especially if the density of the shield is small. Large changes in shape during reentry can alter the drag characteristics of the vehicle and must therefore be eliminated or at least be predicted and planned for.

A complete analysis of the change of shape problem is beyond the scope of this report, however the recession distances at the stagnation and sonic points may be calculated very simply from equations (42a) and (42b). For example, by using the numerical values

$$\frac{V_i^2}{gr} = 1 \qquad \sin\gamma = \frac{1}{2}$$

$$v_f = 0.1 \qquad \frac{c_{p,1}}{c_{p,2}} = \frac{2}{3}$$

$$R = \frac{1}{2} \text{ ft} \qquad \rho_b = 144 \text{ lb/cu ft}$$

$$L + c_b\left(T_a - T_b\right) = 1{,}000 \text{ Btu/lb}$$

the following results are obtained from equations (42a) and (43a):

At the stagnation point,

$$m = 8.38 \text{ lb/sq ft}$$

$$d = 0.7 \text{ in.}$$

At the sonic point,

$$m = 17.95 \text{ lb/sq ft}$$

$$d = 1.5 \text{ in.}$$

The recession distances are shown in figure 4 where the sonic point is considered to be at the 45° position. A sketch of the final shape shows maximum recession of the surface at this position.

DISCUSSION

The foregoing analysis has been concerned with the loss of material from, and the accumulation of heat within, an ablation shield of a ballistic vehicle during reentry. The type of ablation considered is that in which no liquid film is produced, the products of ablation being completely gaseous.

Ballistic reentry has been characterized by the ballistic impact parameter B first introduced in reference 1; this parameter has the physical interpretation

$$B = \frac{\text{Mass of column of air in vehicle path}}{\text{Mass of vehicle}}$$

so that small values of B lead to high impact velocities. It is seen from figure 1 that the impact velocity does not change appreciably with B for values of B greater than 6; however, as B decreases from 6 to 3 (by doubling the vehicle weight, for example, or halving the frontal area) the impact velocity increases from $0.05V_i$ to $0.24V_i$, a factor of nearly 5. The associated total heat input increases, of course, but by less than a factor of 2, as seen from figure 2. The total aerodynamic heat input increases rapidly with impact velocity for values less than $0.05V_i$ (i.e., $B > 6$) but increases only linearly for values of the impact velocity greater than $0.05V_i$ $(B < 6)$, as shown in figure 2.

The first conclusion to be drawn from the analysis is that the radiative heat losses from the shield are negligible compared with the heat disposed by ablation, except for materials having exceedingly high ablation temperatures and for vehicles of low impact velocity. For a vehicle having supersonic impact velocity the reentry time is so short that surface radiation from the vehicle is less than 5 percent of the total heat input, even if the surface operates at a temperature of $4,000^{\circ}$ R throughout reentry. Such a surface temperature would naturally increase the insulation requirements. From this point of view the materials most appropriate for high impact velocity vehicles are those which have fairly low ablation temperatures. The loss of radiative cooling is more than balanced by the reduction in insulation.

L 8 5 6

On the other hand, if the material has simultaneously a high ablation temperature and low enough conductivity, it is possible that the reduction in mass loss due to the lower convective heating rate may offset the increase in insulation. Such a high temperature shield may then be more efficient on an overall weight basis.

The shielding capability of ablation materials has been characterized by a parameter λ, the ratio of internal shielding (the sum of the latent heat and heat-sink capacity) to external shielding (the capacity of the ablation gases to absorb heat during convection). When the gas-layer shielding is predominant ($\lambda \rightarrow 0$) the analysis shows that the mass loss has a limiting value which is independent of the entry and impact velocities and the vehicle parameter $\frac{M}{C_D A}$. The total effective heat capacity is also virtually independent of this latter parameter over a wide range of conditions and may be written:

$$\left(H_{eff}\right)_{lam} = L + c_b\left(T_a - T_b\right) + 8,100\left(\frac{5}{6}\,\frac{c_{p,1}}{c_{p,2}} + \frac{1}{6}\right)\frac{V_i^{\,2}}{gr}\,\bar{G}_{1/2}$$

$$\left(H_{eff}\right)_{turb} = L + c_b\left(T_a - T_b\right) + 4,050\left(\frac{5}{6}\,\frac{c_{p,1}}{c_{p,2}} + \frac{1}{6}\right)\frac{V_i^{\,2}}{gr}\,\bar{G}_{4/5}$$

For the range of conditions presently of interest, $\bar{G}_p$ is approximately constant and equal to 0.6 as is seen from figure 3. As the foregoing expressions indicate, the gas-layer shielding is only one-half as effective at the sonic point as at the stagnation point.

An illustrative calculation with typical numerical values shows that the surface recession is such that the nose may change shape sufficiently to affect the drag characteristics of the vehicle, in the example shown in figure 4, the hemisphere with an initial radius of 6 inches recedes 1.5 inches at the sonic point, compared with 0.7 inch at the stagnation point.

CONCLUDING REMARKS

An analysis of the sublimation of material from a ballistic vehicle shield has been made. The two controlling parameters of the problem are found to be the ballistic impact parameter

$$\frac{\text{Mass of column of air in vehicle path}}{\text{Mass of vehicle}}$$

and the ablation shielding parameter

$$\frac{\text{Internal shielding}}{\text{Gas-layer shielding}}$$

General approximate expressions for the total ablation experienced by the shield at the stagnation and sonic points indicate that the nose may undergo considerable change in shape during reentry. The simplified engineering forms of these expressions applied to a hemispherical nose show the final shape to be indented in the region of the sonic point.

Estimates of the insulation requirements with the use of typical material properties show that insulation weight makes only a secondary contribution to the total weight of the shield.

Langley Research Center,
National Aeronautics and Space Administration,
Langley Field, Va., January 14, 1960.

REFERENCES

1. Lees, Lester: Similarity Parameters for Surface Melting of a Blunt Nosed Body in a High Velocity Gas Stream. ARS Jour., vol. 29, no. 5, May 1959, pp. 345-354.

2. Roberts, Leonard: A Theoretical Study of Stagnation-Point Ablation. NASA TR R-9, 1959. (Supersedes NACA TN 4392.)

3. Roberts, Leonard: Stagnation Point Shielding by Melting and Vaporization. NASA TR R-10, 1959.

4. Bethe, Hans A., and Adams, Mac C.: A Theory for the Ablation of Glassy Materials. Jour. Aero/Space Sci., vol. 26, no. 6, June 1959, pp. 321-328, 350.

5. Allen, H. Julian, and Eggers, A. J., Jr.: A Study of the Motion and Aerodynamic Heating of Ballistic Missiles Entering the Earth's Atmosphere at High Supersonic Speeds. NACA Rep. 1381, 1958. (Supersedes NACA TN 4047.)

6. Chapman, Dean R.: An Analysis of Corridor and Guidance Requirements for Supercircular Entry Into the Earth's Atmosphere. NASA TR R-55, 1960.

7. Roberts, Leonard: An Analysis of Ablation-Shield Requirements for Manned Reentry Vehicles. NASA TR R-62, 1960.

8. Leadon, B. M., and Scott, C. J.: Measurement of Recovery Factors and Heat Transfer Coefficients With Transpiration Cooling in a Turbulent Boundary Layer at M = 3.0 Using Air and Helium as Coolants. Res. Rep. No. 126, Univ. of Minnesota Inst. Tech., Dept. Aero. Eng. (Contract AF 18(600)-1226), Feb. 1956.

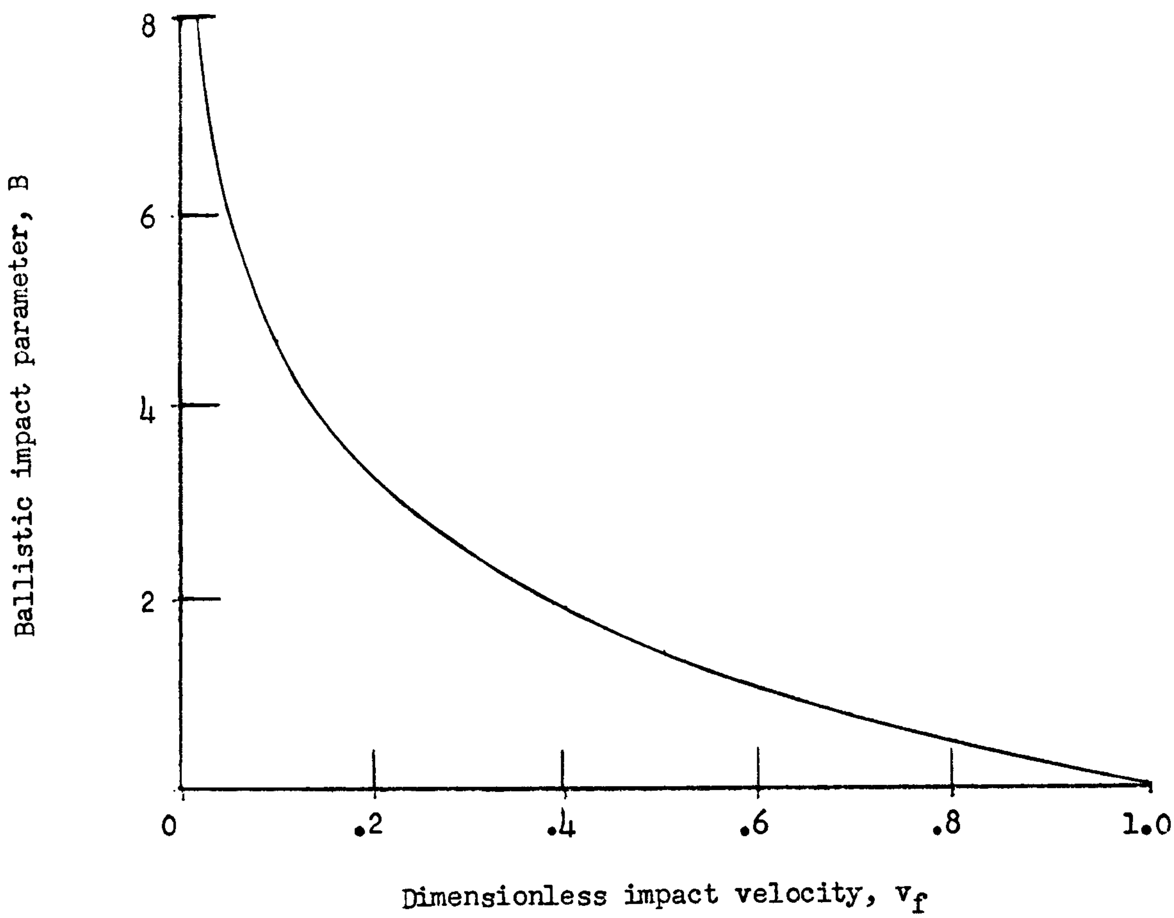

Figure 1.- Variation of ballistic impact parameter B with impact velocity.

L-856

L-856

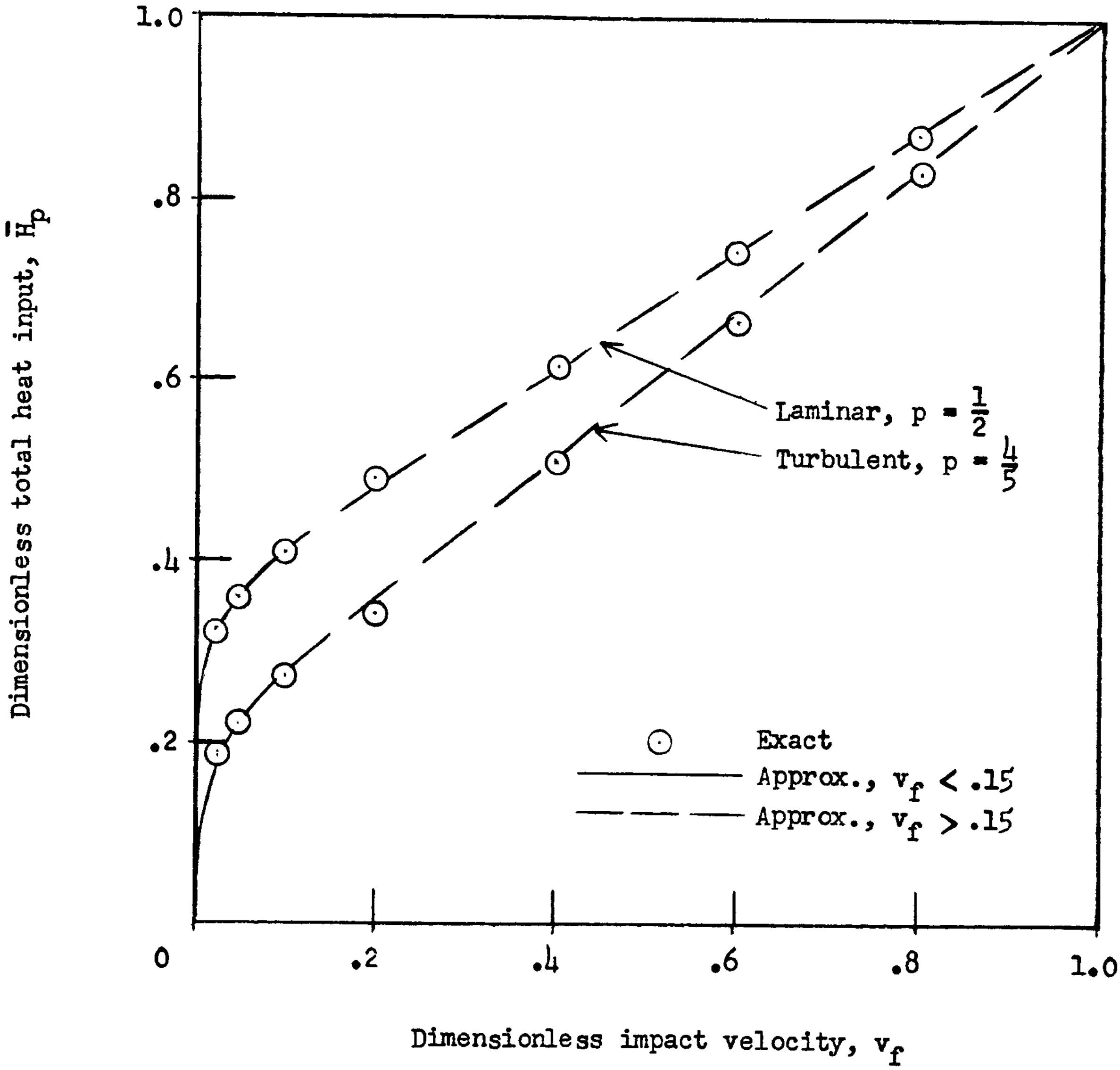

Figure 2.- Variation of total heat input parameter with impact velocity.

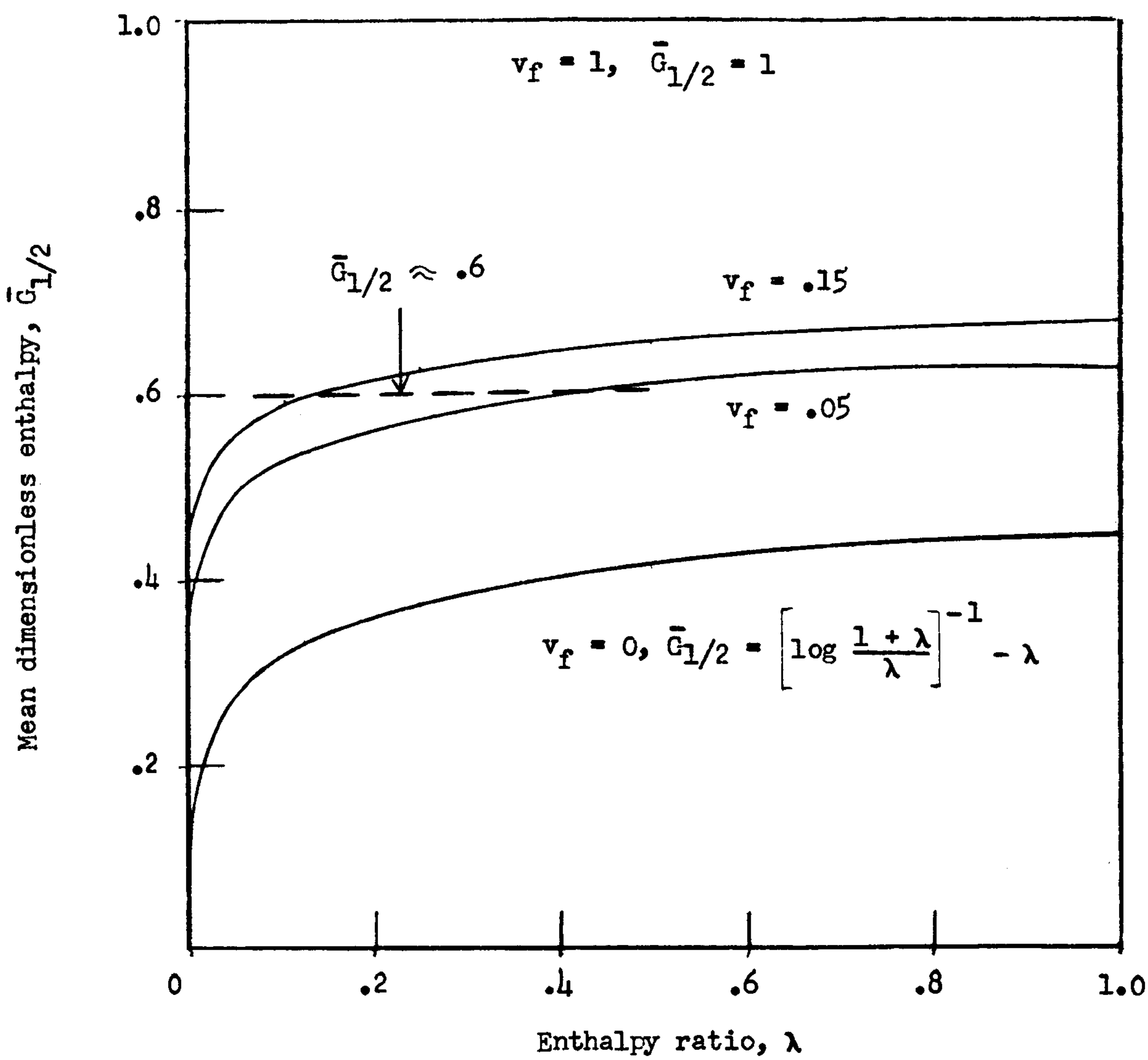

(a) Laminar flow.

Figure 3.- Variation of enthalpy parameter $\bar{G}_p$ with enthalpy ratio λ.

L-856

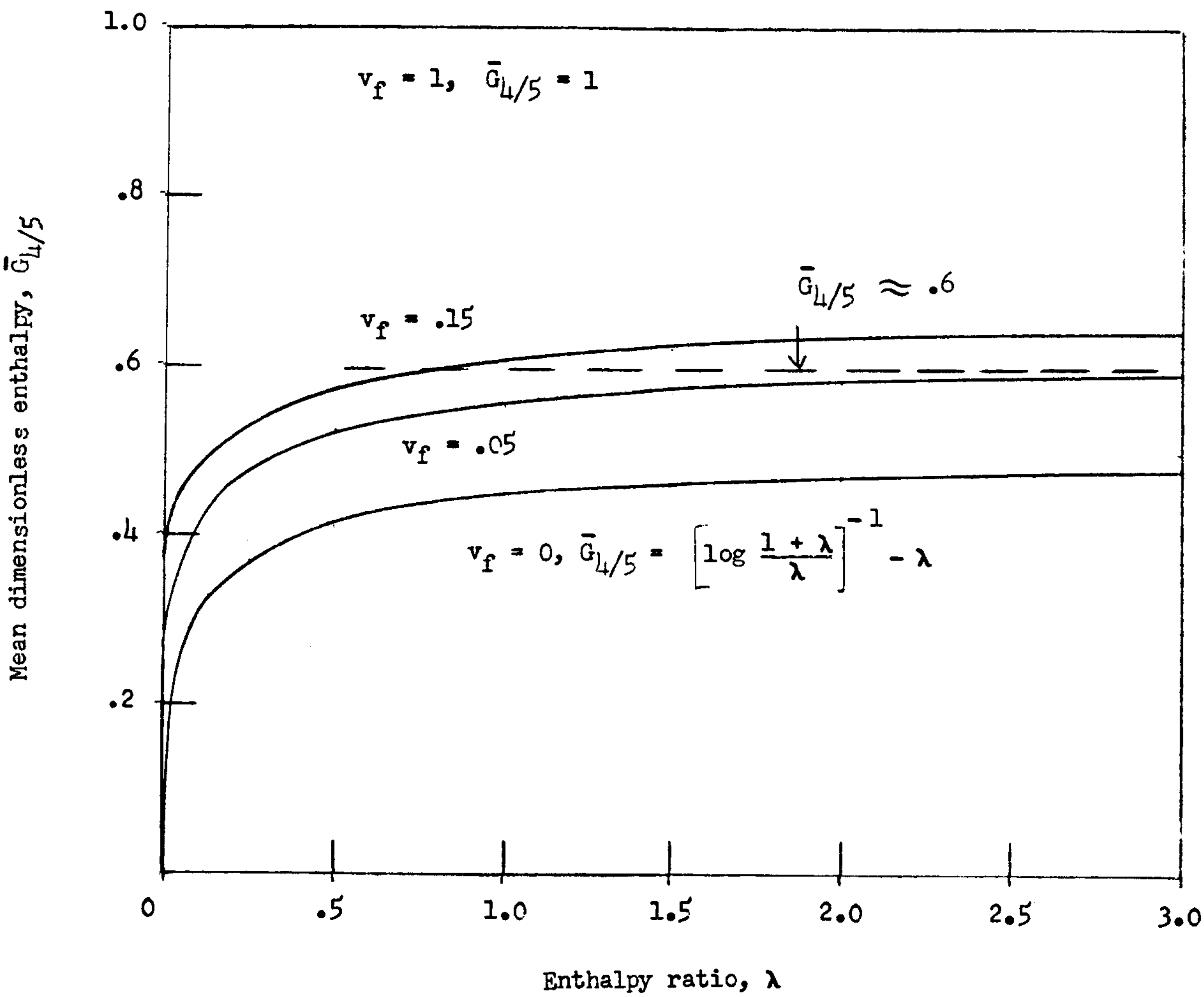

(b) Turbulent flow.

Figure 3.- Concluded.

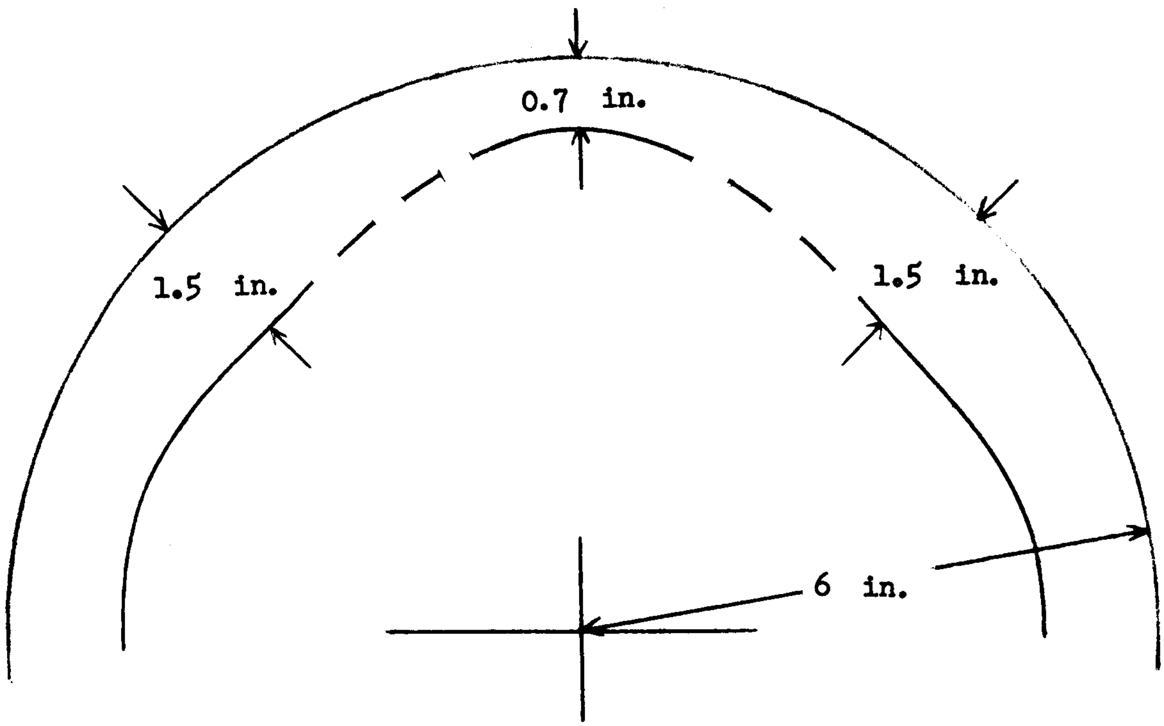

Figure 4.- Change of shape of hemispherical cap during reentry.